VARIABLE STARS AND STELLAR POPULATIONS IN ANDROMEDA XXVII: IV. AN OFF-CENTERED, DISRUPTED GALAXY *

FELICE CUSANO[1], ALESSIA GAROFALO[1,2], GISELLA CLEMENTINI[1], MICHELE CIGNONI[3], TATIANA MURAVEVA[1], GIANNI TESSICINI[1], VINCENZO TESTA[4], DIEGO PARIS[4], LUCIANA FEDERICI[1], MARCELLA MARCONI[5], VINCENZO RIPEPI[5], ILARIA MUSELLA[5]

[1]*INAF- Osservatorio Astronomico di Bologna, Via Gobetti 93/3, I - 40129 Bologna, Italy*

felice.cusano@oabo.inaf.it

[2] *Dipartimento di Fisica e Astronomia, Università di Bologna, viale Berti Pichat, 6/2, I - 40127 Bologna, Italy*

[3] *Dipartimento di Fisica, Università di Pisa, Largo Bruno Pontecorvo, 3, 56127 Pisa PI*

[4]*INAF- Osservatorio Astronomico di Roma, Via di Frascati 33 00040 Monte Porzio Catone, Italy*

[5]*INAF- Osservatorio Astronomico di Capodimonte, Salita Moiariello 16, I - 80131 Napoli, Italy*

ABSTRACT

We present B and V time series photometry of the M31 satellite galaxy Andromeda XXVII (And XXVII) that we observed with the Large Binocular Cameras of the Large Binocular Telescope. In the field of And XXVII we have discovered a total of 90 variables: 89 RR Lyrae stars and 1 Anomalous Cepheid. The average period of the fundamental mode RR Lyrae stars (RRab) $\langle P_{ab}\rangle$=0.59 d (σ=0.05 d) and the period-amplitude diagram place And XXVII in the class of Oosterhoff I/Intermediate objects. Combining information from the color-magnitude diagram (CMD) and the variable stars we find evidence for a single old and metal poor stellar population with [Fe/H]~ -1.8 dex and t$\sim$13 Gyr in And XXVII. The spatial distribution of RR Lyrae and red giant branch (RGB) stars gives clear indication that And XXVII is a completely disrupted system. This is also supported by the spread observed along the line of sight in the distance to the RR Lyrae stars. The highest concentration of RGB and RR Lyrae stars is found in a circular area of 4 arcmin in radius, centered about 0.2 degrees in south-east direction from Richardson et al. (2011) center coordinates of And XXVII. The CMD of this region is well defined with a prominent RGB and 15 RR Lyrae stars (out of the 18 found in the region) tracing a very tight horizontal branch at $\langle V(RR)\rangle$ = 25.24 mag σ= 0.06 mag (average over 15 stars). We show that And XXVII well proposes as a candidate building block of the M31 halo.

Subject headings: galaxies: dwarf, Local Group —galaxies: individual (Andromeda XXVII) —stars: distances —stars: variables: other —techniques: photometric

1. INTRODUCTION

In the Λ-cold dark matter (CDM) scenario, galaxies are formed by hierarchical assembling of

*Based on data collected with the Large Binocular Cameras at the Large Binocular Telescope, PI: G. Clementini

smaller structures (e.g. Bullock & Johnston 2005; Annibali et al. 2016; Stierwalt et al. 2017). The dwarf satellites of the Andromeda galaxy (M31) can help to constrain the origin and the fate of M31. Through the characterization of the resolved stellar populations and the variable stars in these systems it is possible to trace the global context of merging and accretion episodes occurred and still occurring in the M31 environment (Martin et al. 2013).

This is the fourth paper in our series on the M31 satellites based on B and V time-series photometry obtained with the Large Binocular Cameras (LBC) of the Large Binocular Telescope (LBT). Details on the survey and results from the study of Andromeda XIX (And XIX), Andromeda XXI (And XXI) and Andromeda XXV (And XXV) were presented in Cusano et al. (2013, Paper I), Cusano et al. (2015, Paper II) and Cusano et al. (2016, Paper III), respectively. In this paper we report results on the dwarf spheroidal galaxy (dSph) Andromeda XXVII (And XXVII), that was discovered by Richardson et al. (2011) in the context of the PAndAS survey. The galaxy is located near a portion of Andromeda's North-West stream (NW; see Fig. 1 of Richardson et al. 2011). These authors claimed that And XXVII is in the process of being tidally disrupted by M31 and derived only a lower limit of $\geq 757 \pm 45$ kpc for its heliocentric distance due to the difficulty in measuring the magnitude of the galaxy horizontal branch (HB). Ibata et al. (2013) later found that And XXVII is a member of the thin plane of satellites identified in M31 (Great Plane of Andromeda, GPoA, following the definition of Pawlowski et al. 2013). The heliocentric distance of And XXVII was revised using tip of the Red Giant Branch (RGB) stars by Conn et al. (2012) who estimated a value of 1255^{+42}_{-474} kpc that would place the galaxy outside the M31 complex. The RGB tip of And XXVII is very scarcely populated likely due to the disrupting nature of the galaxy. This may have significantly affected Conn et al. (2012) determination of distance. Collins et al. (2013) measured a metallicity for And XXVII of [Fe/H]$= -2.1 \pm 0.5$ dex estimated from the Calcium triplet (CaII) in eleven probable member stars. The radial velocity of And XXVII measured by the same authors is: $v_r = -539.6$ km s^{-1} with $\sigma = 14.8$ km s^{-1}. Collins et al. (2013) warned that given the disrupting nature of the object, their estimate is very uncertain. They also identified a significant kinematic substructure around ~ -500 km s^{-1}. Very recently Martin et al. (2016) from a re-analysis of the PAndAS data stated that And XXVII is likely a system that is in the final phase of tidal disruption. The wide-field LBT observations of And XXVII presented in this paper lend further support to this evidence from the analysis of both color magnitude diagram (CMD) and spatial distribution of the variable stars.

The paper is organized as follows: Section 2 describes the data collection and processing, Section 3 describes the identification of the variable stars and their characterization. The galaxy CMD is presented in Section 4. Distance and galaxy structure are discussed in Sections 5 and 6. Conclusions are provided in Section 7.

2. OBSERVATIONS AND DATA REDUCTION

Time series observations in the B and V bands of the field around the center coordinates of And XXVII (R.A.=$00^{\rm h}37^{\rm m}27^{\rm s}$, decl.=$+45°23'13''$; J2000, Richardson et al. 2011) were carried out in October-November 2011 (see Table 1 for the complete log) at the LBT equipped with the LBC. The total LBC's field of view (FoV) covers an area of $\sim 23' \times 23'$. Observations were obtained under good sky and seeing conditions (see Table 1). The blue camera (LBC-B) was used to acquire the B images, while V imaging was obtained with the red camera (LBC-R). Bias, flat fielding and distortion corrections of the raw frames were performed with a dedicated pipeline developed at INAF-OAR[1]. We performed PSF photometry of the pre-processed images using the `DAOPHOT - ALLSTAR - ALLFRAME` packages (Stetson 1987, 1994) as described in Paper I. Photometric calibration was performed using the Landolt standard fields L92 and SA113, observed during the same observing run. The calibration equations[2] are consistent with those derived in Paper I, once differences in air-mass and exposure times are accounted for.

[1] *http://lbc.oa-roma.inaf.it/commissioning/index.html*

[2] $B - b = 27.696 - 0.113 \times (b - v)$ r.m.s=0.03,
$V - v = 27.542 - 0.060 \times (b - v)$ r.m.s=0.03

Table 1: Log of And XXVII observations

Dates	Filter	N	Exposure time (s)	Seeing (FWHM) (arcsec)
October 20-24, 2011	B	87	400	0.8-1
November 27-28, 2011	B	5	400	0.8-1
October 20-24, 2011	V	86	400	0.8-1
November 27-28, 2011	V	4	400	0.8-1

3. VARIABLE STARS

Variable stars were identified in our photometric catalogs using the same procedure as described in Paper I. We used the variability index computed in DAOMASTER (Stetson 1994) to search for variable sources. We selected as candidate variables, stars with a variability index (VI) > 1.4, based on our previous experience with other M31 satellites (And XIX, And XXI, And XXV) and LBT photometry. The average value for non variable stellar objects placed on the horizontal branch (HB) and satisfying the quality parameters, $\chi \leq 1.5$, $-0.35 <$ Sharpness < 0.35 (see Section 4), is $\langle \mathrm{VI} \rangle = 1.03$, $\sigma = 0.12$. The value of VI used to select candidate variable stars is thus 3 σ above the average value for HB non variable stars. The selection of variable stars was performed on the photometric catalog for objects satisfying to the quality parameters (χ and Sharpness) mentioned above. The total number of candidate variables that passed our selection criteria is 754. The B and V light curves of the candidate variables were then analyzed using the Graphical Analyzer of Time Series package (GRaTIS), custom software developed at the Bologna Observatory by P. Montegriffo (see, e.g., Clementini et al. 2000). From this analysis, 90 sources were confirmed to vary. Of them 89 are classified as RR Lyrae stars and one as Anomalous Cepheid (AC), based on the pulsation properties and the position in the CMD. The lowest value of VI for a bona fide RR Lyrae stars identified in this work is VI=1.52, hence the VI limit we chose to select candidate variable stars is loose enough to ensure we did not miss candidate variable. Therefore, the completeness of our RR Lyrae stars catalog is mostly driven by the photometric completeness at the HB level. This

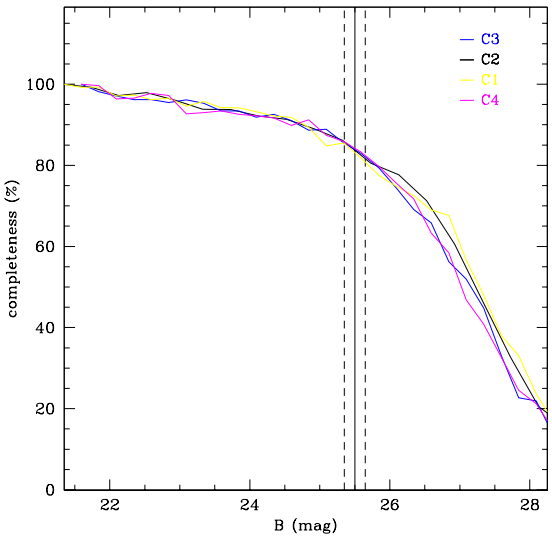

Fig. 1.— Completeness of the photometric catalogs in the four CCDs (hereinafter C1, C2, C3 and C4) of the LBC mosaic. The blue line is C3, the yellow line is C1, the magenta line is C4 and the black line is C2. The vertical solid line marks the average B magnitude of the RR Lyrae stars, dashed lines are the 1 σ boundaries.

was estimated using artificial star test and at the level of HB is $\sim$ 83% as shown in Figure 1. The Figure shows the trend of the completeness in the B-band magnitude for each of the four CCDs of the LBC mosaic, clearly there is no significant difference among the four CCDs especially at the average magnitude of the RR Lyrae stars (solid vertical line). Finally the incompleteness of our RR Lyrae stars catalog is of $\sim$ 17% hence we are probably missing from 10 to 20 RR Lyrae stars in And XXVII field.

Coordinates and properties of the confirmed variable stars are listed in Table 2 where column 1 gives the star identifier; columns 2 and 3 are, respectively, the right ascension and declination (J2000.0 epoch) obtained from our astrometrized catalogs; column 4 provides the type of variability with a question mark identifying stars whose classification is uncertain; columns 5 and 6 give, respectively, the period and the Heliocentric Julian Day (HJD) of maximum light; columns 7 and 9 are the intensity-averaged mean B and V magnitudes; columns 8 and 10 list the corresponding amplitudes of light variation. Examples of light curves, in both filters, are shown in Figure 2. Observations have been performed in five consecutive nights in October and two consecutive nights in November. The data are mostly biased by the one day alias due to the alternation of night-day observations and are thus marginally affecting the period determination of the RR Lyrae stars that in all cases is < 1 day. The full catalog of light curves is available in the electronic version of the paper.

3.1. RR LYRAE STARS

In the field of And XXVII we have discovered a total of 89 RR Lyrae stars, of which 58 are fundamental mode (RRab) and 31 are first-overtone (RRc) pulsators according to period and amplitude of light variation. RR Lyrae stars are excellent tracers of an old stellar population (e.g. Clementini 2010; Marconi et al. 2015, and references therein). Their presence in And XXVII shows that this galaxy started forming stars $\geq$ 10 Gyr ago. The spatial distribution of the variable stars discovered in the FoV of And XXVII is shown if Figure 3. The highest concentration of RR Lyrae stars occurs in CCD3 (labeled C3 in the figure) where there are 32 RR Lyrae to compare with 28 in C2, 21 in C1 and 7 in C4. Furthermore, the very sparse spatial distribution of these variable stars suggests that And XXVII is in the phase of tidal disruption, as the RR Lyrae stars are spread all over the LBC FoV. However, given the proximity to M31 we cannot rule out that some of these RR Lyrae stars might belong to Andromeda's halo. To estimate how many M31 halo RR Lyrae stars we can expect in the LBC FoV centered on And XXVII we considered a number of different arguments. First of all we assumed the surface density profile from Ibata et al. (2013). Despite the complexity of the M31 halo, Ibata et al. (2013) found that the azimuthally-averaged projected star-count-profile for stars in the metallicity range $-2.5 < [Fe/H] < -1.7$ does not have particular features and posses a power-law of $\Gamma = -2.3 \pm 0.02$. Then we considered that Jeffery et al. (2011) found five and no RR Lyrae stars in two HST/ACS field at a distance of 35 kpc from the M31 center. If we apply Ibata et al. power law to the sample of RR Lyrae stars found by Jeffery et al. (2011) after rescaling for the different area surveyed by our LBC images (~ 0.15 deg^2) and the HST/ACS (~ 0.008 deg^2) and the different distance to the center of M31 (the projected distance to And XXVII is 60 kpc), we find a possible contamination of $\sim$ 14 RR Lyrae stars from the M31 halo in And XXVII's LBC field. However, we note that the number of contaminant RR Lyrae stars can be larger than this estimate as And XXVII lies in a region of the M31 halo where stars in the metallicity range $-2.5 < [Fe/H] < -1.7$ form streams and are all around And XXVII, as shown in Figure 9 of Ibata et al. (2014). Thus decontamination of And XXVII stars from field objects is a difficult task.

The period distribution of the RR Lyrae stars identified in the field of And XXVII is shown by the histogram in Figure 4. The average period of the 58 RRab stars is $\langle \mathrm{P_{ab}} \rangle$=0.59 d ($\sigma$=0.05 d), while for the 31 RRc's is $\langle \mathrm{P_c} \rangle$=0.35 d ($\sigma$=0.04 d). Considering that $\sim$ 14 RR Lyrae stars could belong to the M31 halo we performed a bootstrap re-sampling of the data, removing a total of 14 RR Lyrae stars. Among the 14 we removed randomly 9 RRab and 5 RRc, consistently to the fraction of RRc over total RR Lyrae stars found. Both average period and related σ of RRab and RRc stars, separately, do not change significantly, giving us confidence that the RR Lyrae stars of And XXVII have the same properties of those belonging to the surrounding M31 halo.

Based on the average period of the fundamental-mode pulsators, And XXVII would be classified as an Oosterhoff-Intermediate (Oo Int)/OoI system (Oosterhoff 1939; Catelan 2009), however, we note that And XXVII has the lowest value of $\langle \mathrm{P_{ab}} \rangle$ among the four M31 satellites we have investigated so far based on LBT data. The frac-

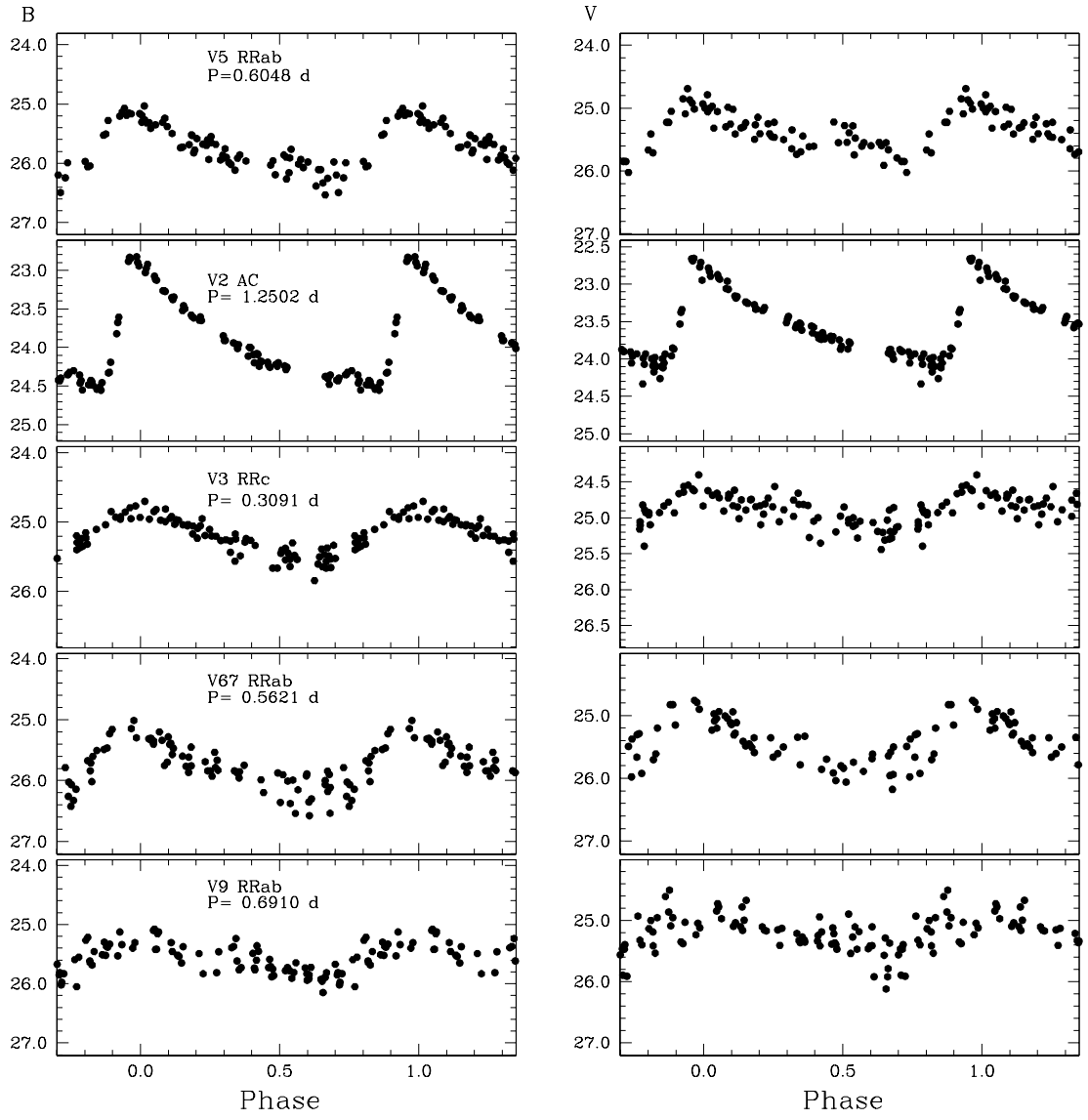

Fig. 2.— Examples of B- (left panels) and V-band (right panels) light curves for different types of variable stars identified in And XXVII (from top to bottom: fundamental-mode RR Lyrae star, anomalous Cepheid, first overtone RR Lyrae star, V67 the only fundamental-mode RR Lyrae star with $D_m < 3$ and V9 the RRab with the highest D_m value). Typical internal errors of the single-epoch data range from 0.01 at $B \sim 22.8$ mag (corresponding to the maximum light of the AC) to 0.30 mag at $B \sim 26.8$ mag (corresponding to the minimum light of a fundamental mode RR Lyrae), and similarly, from 0.01 mag at $V \sim 22.6$ mag to 0.30 mag at $V \sim 26.8$ mag.

Table 2: Identification and properties of the variable stars detected in And XXVII.

Name	α (2000)	δ (2000)	Type	P (days)	Epoch (max) HJD (-2455000)	$\langle B \rangle$ (mag)	A_B (mag)	$\langle V \rangle$ (mag)	A_V (mag)
V1	00:37:31.893	+45:23:54.12	RRab	0.6171	53.792	25.38	0.62	24.94	0.49
V2	00:37:32.950	+45:22:58.27	AC	1.2502	53.085	23.79	1.73	23.48	1.43
V3	00:37:33.655	+45:24:40.61	RRc	0.3091	53.633	25.19	0.74	24.91	0.53
V4	00:37:19.667	+45:24:27.33	RRc	0.3857	53.272	25.38	0.82	25.08	0.59
V5	00:37:36.643	+45:22:58.03	RRab	0.6048	54.080	25.72	1.05	25.37	0.82
V6	00:37:19.271	+45:21:17.88	RRc	0.3642	53.600	25.61	0.59	25.32	0.46
V7	00:37:28.721	+45:26:12.74	RRab	0.5798	53.762	25.78	1.04	25.25	0.55
V8	00:37:25.769	+45:19:50.86	RRab	0.5999	53.421	25.55	0.94	25.14	0.62
V9	00:37:22.045	+45:26:39.96	RRab	0.6910	53.292	25.56	0.66	25.19	0.66
V10	00:37:23.724	+45:19:30.90	RRab	0.6226	53.817	25.74	0.52	25.33	0.37
V11	00:37:16.889	+45:26:08.05	RRc	0.3552	53.428	25.41	0.69	25.06	0.42
V12	00:37:19.295	+45:19:31.97	RRc	0.2432	53.856	25.30	0.69	25.05	0.57
V13	00:37:37.243	+45:27:03.68	RRc	0.3635	53.735	25.38	0.72	24.99	0.53
V14	00:37:38.799	+45:26:48.76	RRab	0.6710	53.271	25.22	0.94	24.76	0.70
V15	00:37:44.006	+45:21:10.15	RRab	0.5645	53.783	25.78	0.97	25.53	0.85
V16	00:37:21.577	+45:18:40.74	RRab	0.5881	53.459	25.72	1.16	25.35	0.78
V17	00:37:46.582	+45:23:51.84	RRab	0.6586	53.390	25.64	0.67	25.30	0.59
V18	00:37:29.435	+45:28:15.86	RRab	0.5793	53.425	25.57	1.09	25.21	0.89
V19	00:37:30.249	+45:18:03.82	RRab	0.6181	53.987	25.33	1.30	25.05	1.18
V20	00:37:07.677	+45:26:04.87	RRab	0.5612	53.679	25.30	1.49	24.92	0.99
V21	00:37:40.518	+45:27:58.79	RRc	0.4357	53.691	25.42	0.46	24.99	0.31
V22	00:37:12.966	+45:18:22.55	RRc	0.2925	53.985	25.33	0.67	25.12	0.57
V23	00:37:38.962	+45:28:28.95	RRab	0.5570	53.857	25.11	1.14	24.70	0.96
V24	00:37:06.459	+45:19:45.37	RRab	0.5746	53.559	25.41	1.19	25.10	0.96
V25	00:37:45.060	+45:18:43.87	RRab	0.7150	53.391	25.52	0.71	25.11	0.70
V26	00:37:01.535	+45:24:21.95	RRab	0.5535	53.588	25.66	1.00	25.26	1.03
V27	00:37:45.003	+45:28:36.34	RRc	0.3938	53.147	25.52	0.56	25.10	0.35
V28	00:37:52.395	+45:19:57.61	RRab	0.5870	53.910	25.58	0.95	25.13	0.87
V29	00:37:17.317	+45:30:03.48	RRc	0.3601	54.076	25.34	0.44	24.88	0.38
V30	00:36:59.737	+45:25:39.13	RRab	0.5541	53.887	25.50	1.04	25.14	0.69
V31	00:37:56.368	+45:25:06.03	RRab	0.5408	53.803	25.56	1.05	25.25	0.98
V32	00:37:57.393	+45:21:23.21	RRc?	0.2793	53.931	25.44	0.47	25.27	0.47
V33	00:37:56.332	+45:20:25.79	RRab	0.5492	53.824	25.50	0.82	25.23	0.50
V34	00:37:00.936	+45:18:26.79	RRab	0.5579	53.875	25.54	1.46	25.18	1.00
V35	00:37:58.868	+45:20:16.64	RRc	0.3579	53.544	25.67	0.58	25.30	0.43
V36	00:38:00.070	+45:21:13.33	RRc	0.3641	53.781	25.60	0.66	25.21	0.67
V37	00:38:00.481	+45:24:46.02	RRab	0.5996	53.525	25.35	1.31	24.99	0.96
V38	00:37:52.645	+45:17:32.73	RRc	0.3987	53.928	25.27	0.63	24.92	0.45
V39	00:36:55.883	+45:27:09.36	RRc	0.3534	53.504	25.51	0.82	25.14	0.56
V40	00:38:02.723	+45:24:46.06	RRc	0.3395	53.616	25.50	0.72	25.28	0.59
V41	00:37:13.142	+45:14:50.52	RRab	0.5888	53.486	25.50	1.05	25.20	1.02
V42	00:36:51.394	+45:25:50.83	RRc	0.3550	53.660	25.55	0.57	25.27	0.56
V43	00:37:56.003	+45:29:09.95	RRab	0.6087	53.686	25.66	0.97	25.24	0.72
V44	00:37:25.859	+45:32:50.55	RRab?	0.6312	53.322	25.37	0.45	25.12	0.53
V45	00:36:49.108	+45:20:47.83	RRab	0.5315	53.758	25.37	1.28	25.03	1.18
V46	00:37:24.064	+45:13:16.69	RRab	0.5855	54.116	25.78	0.82	25.46	0.90
V47	00:38:02.920	+45:18:20.73	RRab	0.5293	53.342	25.67	1.14	25.29	0.70
V48	00:38:06.624	+45:20:36.47	RRc	0.3501	53.816	25.58	0.54	25.26	0.45
V49	00:38:05.333	+45:19:20.00	RRc	0.3541	53.015	25.54	0.50	25.21	0.31
V50	00:36:48.952	+45:19:02.07	RRab	0.6451	53.359	25.56	1.17	25.14	0.76
V51	00:37:13.308	+45:13:20.85	RRc	0.3558	53.410	25.53	0.61	25.28	0.51
V52	00:36:47.422	+45:27:31.80	RRab	0.5627	53.761	25.20	1.21	24.84	0.85
V53	00:36:52.857	+45:30:18.98	RRab	0.5980	53.706	25.42	0.78	25.06	0.69
V54	00:38:11.223	+45:21:26.58	RRab	0.5754	54.079	25.41	1.10	25.12	1.02
V55	00:37:09.934	+45:12:53.19	RRab	0.6226	53.920	25.53	0.79	25.24	0.57
V56	00:38:02.164	+45:30:14.28	RRab	0.5794	53.853	25.60	0.95	25.26	0.84
V57	00:36:42.634	+45:21:18.38	RRab	0.5357	53.638	25.49	1.18	25.29	0.96
V58	00:38:10.002	+45:18:59.73	RRab	0.5395	53.369	25.62	1.00	25.25	0.79
V59	00:37:43.102	+45:34:14.31	RRab	0.6000	53.707	25.42	1.19	25.04	0.92
V60	00:36:39.192	+45:23:25.77	RRab	0.5788	53.866	25.47	0.94	25.09	0.94
V61	00:38:16.025	+45:24:01.56	RRc?	0.3830	53.841	25.43	0.75	25.20	0.76
V62	00:36:37.523	+45:23:46.74	RRc	0.4281	53.797	25.41	0.58	24.95	0.22
V63	00:38:15.170	+45:19:44.42	RRab	0.6023	53.829	25.10	0.87	24.73	0.71
V64	00:36:42.559	+45:17:17.99	RRab	0.5537	53.877	25.41	1.19	25.10	0.96
V65	00:38:07.107	+45:31:17.21	RRab	0.6035	53.411	25.57	0.87	25.16	0.53
V66	00:38:17.987	+45:21:20.02	RRab	0.7383	53.309	25.34	0.52	24.77	0.35
V67	00:38:14.697	+45:17:42.86	RRab	0.5621	53.544	25.76	0.90	25.45	0.68
V68	00:36:45.329	+45:14:56.17	RRc	0.3682	53.304	25.49	0.67	25.21	0.50
V69	00:38:13.766	+45:16:28.40	RRab	0.5715	53.933	25.70	0.90	25.33	0.98
V70	00:36:33.155	+45:24:24.17	RRc	0.3547	53.748	25.54	0.58	25.15	0.37
V71	00:38:20.719	+45:20:47.63	RRc	0.3594	53.929	25.45	0.66	25.15	0.58
V72	00:38:18.355	+45:27:54.69	RRab	0.6236	53.679	25.64	0.84	25.25	0.71
V73	00:38:06.155	+45:32:45.88	RRab	0.6524	53.969	25.57	1.22	25.27	1.16
V74	00:38:12.060	+45:15:24.61	RRab	0.5616	53.699	25.56	0.96	25.12	0.56
V75	00:38:05.872	+45:13:29.96	RRc	0.3487	53.877	25.50	0.64	25.20	0.56
V76	00:36:35.681	+45:28:17.18	RRc	0.3642	53.833	25.53	0.65	25.20	0.48
V77	00:38:23.292	+45:22:27.00	RRab	0.5306	53.267	25.65	1.15	25.30	0.96
V78	00:38:14.075	+45:15:18.82	RRc	0.3333	53.837	25.50	0.68	25.24	0.65
V79	00:36:29.952	+45:23:43.59	RRc?	0.2924	53.494	25.37	0.70	25.19	0.48
V80	00:38:23.752	+45:20:48.11	RRc	0.3648	53.352	25.61	0.74	25.31	0.64
V81	00:36:30.046	+45:25:46.60	RRab	0.5595	53.968	25.26	1.01	24.89	0.82
V82	00:38:09.009	+45:12:59.08	RRc	0.2547	53.786	25.49	0.69	25.24	0.38
V83	00:38:27.464	+45:23:03.51	RRab	0.5628	53.780	25.50	1.15	25.16	0.92
V84	00:36:31.312	+45:28:59.64	RRab	0.6628	53.385	25.33	1.00	24.83	0.71
V85	00:38:20.435	+45:15:59.67	RRab	0.5575	53.929	25.87	1.38	25.48	1.11
V86	00:38:28.400	+45:20:51.17	RRab	0.5453	54.120	25.73	1.10	25.29	0.99
V87	00:36:28.323	+45:15:54.01	RRab	0.7117	53.641	25.45	0.77	25.10	0.56
V88	00:38:32.760	+45:26:30.92	RRab	0.6063	53.786	25.47	0.73	25.07	0.56
V89	00:36:19.903	+45:21:49.53	RRab	0.5905	53.809	25.29	1.68	25.01	1.47
V90	00:36:21.505	+45:18:27.19	RRab	0.5959	53.657	25.41	1.03	25.15	0.64

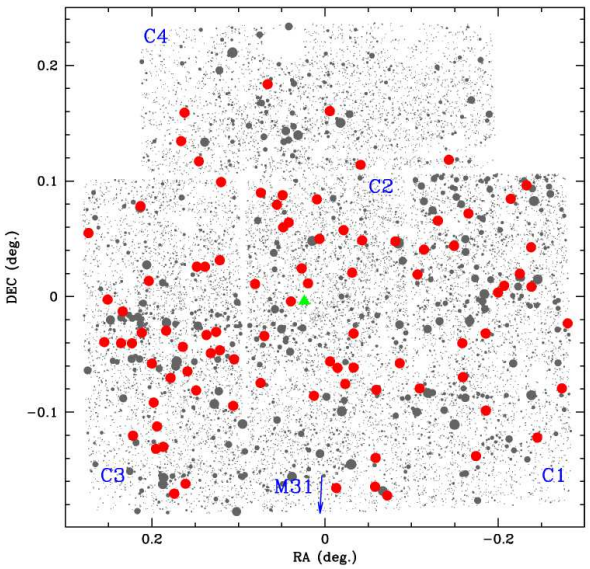

Fig. 3.— Spatial distribution of the variable stars discovered in the whole LBT FoV. The 4 CCDs of the LBC mosaic are labeled. Red filled circles mark the RR Lyrae stars, the green filled triangle is the AC. Gray points are non variable sources, selected as to have DAOPHOT quality image parameters: $-0.35 \leq$ Sharpness ≤ 0.35 and $\chi < 1.5$. Their size is inversely proportional to the source V-magnitude. Contamination by MW sources and background galaxies has not been removed (see Section 4). There are 32 RR Lyrae stars displayed in C3, 28 in C2, 21 in C1 and 7 in C4. The blue arrow points to the direction of M31. North is up, east to the left.

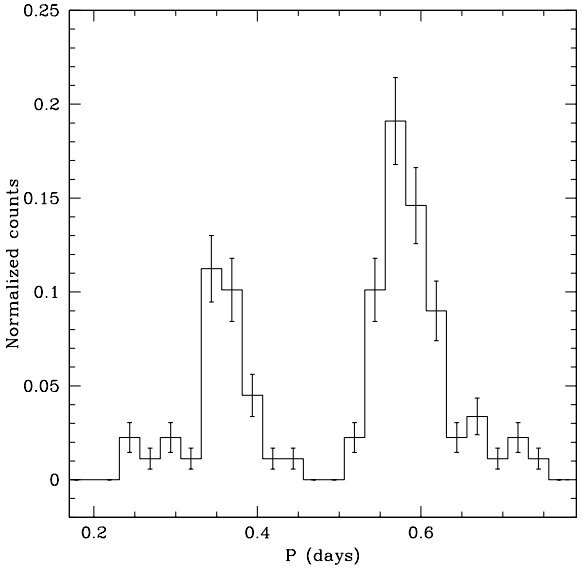

Fig. 4.— Period distribution of the RR Lyrae stars identified in the field of And XXVII. The bin size is 0.025 days.

tion of RRc to total number of RR Lyrae stars is $f_c = N_c/N_{ab+c} = 0.35 \pm 0.07$. This is much closer to the value expected for Oosterhoff II (Oo II; $f_c \sim 0.44$) than Oosterhoff I (Oo I; $f_c \sim 0.17$) systems (Catelan 2009). Even in the extreme case that 5 RRc variables belong to the M31 halo and all the RRab stars to And XXVII the fraction would become f_c=0.30 that is still rather high for an Oo I system. Hence, while the average period of the RRab stars suggests a classification as Oo-Int/Oo I type, the RRc fraction would suggest a classification more similar to Oo II type. The left panel of Figure 5 shows the period-amplitude diagram (also known as Bailey diagram, Bailey 1902) of the RR Lyrae stars in And XXVII. Solid lines are the loci defined by RR Lyrae stars in the Oo I Galactic globular cluster M3 (lower line) and the Oo II globular cluster ω Cen (upper line), according to Clement & Rowe (2000). The majority of the RR Lyrae stars in And XXVII are placed near the locus of the Oo I systems and there are no differences among RR Lyrae stars located in different parts of the LBC FoV (see Sections 4, 5 and Table 3). We conclude that the $\langle P_{ab} \rangle$ value and the Bailey diagram suggest a classification as OoI/Int system for And XXVII.

3.2. Metallicity

Metallicities for the RRab stars in And XXVII were derived using the relation of Alcock et al. (2000; see their Equation 1). The resulting metallicity distribution is shown in Figure 6. A gaussian fit of this distribution peaks at [Fe/H]= −1.62 dex (σ=0.23 dex). This value is consistent with the photometric estimate of [Fe/H]=-1.7 ± 0.2 dex obtained in the discovery paper (Richardson et al. 2011) by isochrone fitting of the galaxy CMD, and is within 1 σ from the spectroscopic estimate of [Fe/H]=-2.1 ± 0.5 dex by Collins et al. (2013). A photometric estimate of the RR Lyrae metallic-

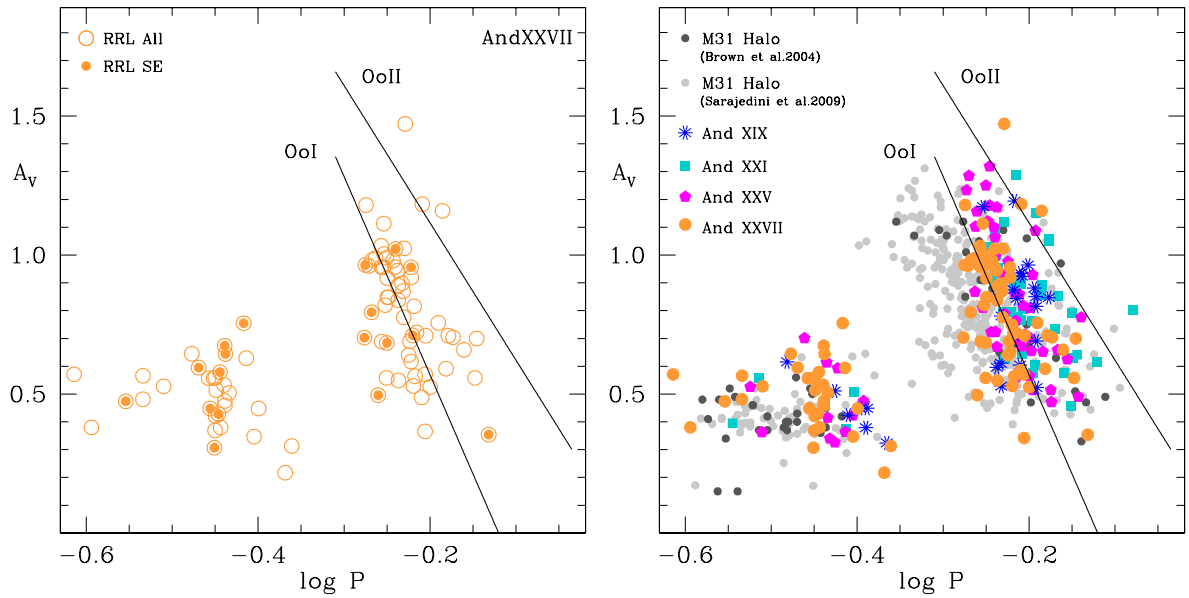

Fig. 5.— *Left*: Period-amplitude diagram of the RR Lyrae stars in the field of And XXVII (orange open circles), highlighted with filled orange circles are those located in the SE region (see Section 4). The two solid lines show the loci defined by Oo I and Oo II RR Lyrae stars according to Clement & Rowe (2000). *Right*: Period-amplitude diagram of the RR Lyrae stars in the field of And XXVII (orange filled circles) compared with the RR Lyrae stars in And XIX (blue asterisks, from Paper I), And XXI (cyan squares, from Paper II)), And XXV (magenta pentagons, from Paper III)) and in three HST fields in the M31 halo from Sarajedini et al. (2009; gray dots) and Brown et al. (2004, dark-gray dots), respectively.

ity can also be derived from the ϕ_{31} parameter of the Fourier decomposition of the light curve (see, e.g., Simon & Teays 1982, Jurcsik & Kovacs 1996, Cacciari et al. 2005). We performed a sine Fourier decomposition of the V-band light curves of the RRab stars in our sample deriving the normalized Fourier parameter ϕ_{31} and the deviation parameter D_m, which measures the regularity of the light curve (Jurcsik & Kovacs 1996). According to Jurcsik & Kovacs (1996) a reliable metallicity can be estimated from the ϕ_{31} parameter only if the light curve satisfies the condition $D_m < 3$.

Among the RRab stars in our sample only V67 satisfies this condition.[3] The light curve of V67 is shown in Figure 2. We applied Equation 3 in Jurcsik & Kovacs (1996) and derived the metallicity $[\mathrm{Fe/H}]_{\mathrm{JK96}} = -1.75 \pm 0.49$ dex on the Jurcsik & Kovacs metallicity scale, which becomes $[\mathrm{Fe/H}]_{\mathrm{C09}} = -1.86 \pm 0.50$ dex once transformed to the Carretta et al. (2009) metallicity scale using Equation 3 from Kapakos et al. (2011). All these values are consistent within their errors with the peak value of the distribution obtained applying Alcock et al.'s method (see Figure 6).

3.3. THE ANOMALOUS CEPHEID

One of the variable stars identified in And XXVII (V2) falls in the instability strip about one magnitude brighter than the galaxy HB level (see Figure 9). Following the same procedure adopted in Paper I we have compared V2 with the period-Weseneheit (PW) relations of Large Magellanic Cloud (LMC) ACs from Ripepi et al. (2014)[4] and the PW relations of LMC classical Cepheids

[3] According to Cacciari et al. (2005) variables satisfying the relaxed condition $D_m < 5$ could also be used. There are three RR Lyrae stars with $3 < D_m < 5$. They provide very scattered and unreliable metallicity values hence we did not consider them.

[4] Ripepi et al. (2014)'s relations were derived for the V and I bands, and we have converted them to B and V using equation 12 of Marconi et al. (2004).

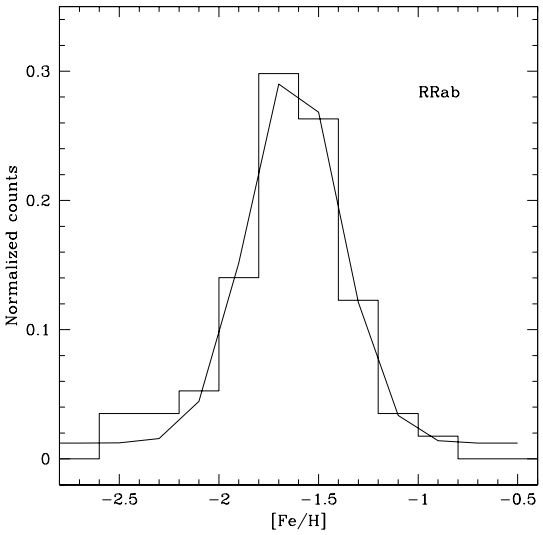

Fig. 6.— Metallicity distribution of And XXVII RRab stars obtained using Alcock et al.(2000) method. The distribution peaks at [Fe/H]~ -1.62 with $\sigma \sim 0.23$ dex.

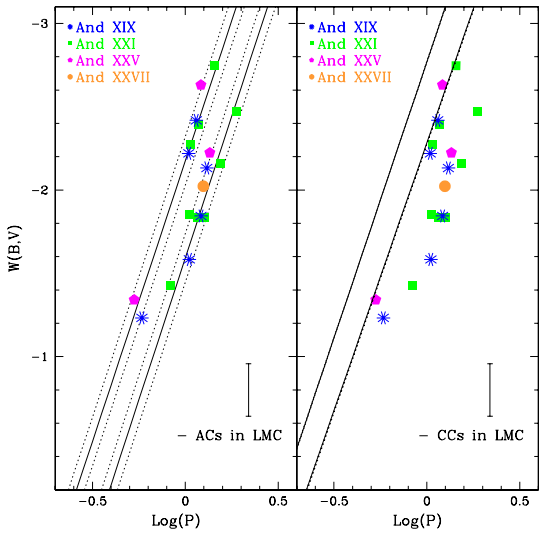

Fig. 7.— Position on the PW plane of star V2 (orange filled circle). Solid lines represent the PW relations for ACs (left panel; Ripepi et al. 2014) and CCs in the LMC (right panel; Jacyszyn-Dobrzeniecka et al. 2016), respectively. Blue, green and magenta symbols are ACs we have identified in And XIX (Paper I), And XXI (Paper II), and And XXV (Paper III). The dotted lines show the $\pm 1\sigma$ deviations. For the CCs the errors of the fits are very small and the confidence contours are very close to the fits.

(CCs) from Jacyszyn-Dobrzeniecka et al. (2016). These comparisons are shown in the left and right panels of Figure 7, respectively, that were drawn assuming for And XXVII the distance inferred from the RR Lyrae stars (see Section 5). We have also plotted in the two panels of Figure 7 the ACs we have identified in And XIX, And XXI, and And XXV.

Figure 7 shows that V2 well follows the PW relation for fundamental mode ACs, while it can be definitely ruled out that the star is a short period CC (see right panel of Figure 7). The AC in And XXVII can be interpreted as the result of a merging in a binary system as old as the RR Lyrae stars in which mass transfer acted in the last 1-2 Gyr. The single young star scenario can be excluded considering that in the CMD there is no evidence of a young stellar component (see Section 4).

As in previous papers of this series, we computed the specific frequency of ACs in And XXVII assuming that V2 is the only AC in the galaxy and compared it with results for other galaxies. This is shown in Figure 8, where the AC specific frequencies of other Milky Way (MW; blue filled circles) and M31 (green and red filled squares) satellites are taken from Paper III. The blue ridge line shows the relation obtained from all the dwarf satellites in the plot. The M31 satellites that are off the GPoA (red squares) seem to follow a different trend shown by the red dashed line. The sample is still statistically too poor to conclude that off- and on-plane satellites obey to different correlations between ACs specific frequency and luminosity or metallicity, but the satellites studied so far seem to suggest that this may be the case.

4. CMD AND PROJECTED SPATIAL DISTRIBUTIONS

The CMD of the sources in the whole LBC FoV is presented in Figure 9. Only sources with DAOPHOT quality image parameters: $-0.35 \leq$ Sharpness ≤ 0.35 and $\chi < 1.5$ are displayed. The

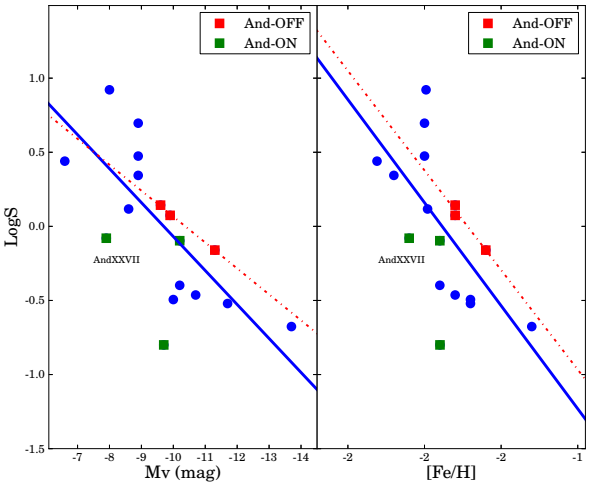

Fig. 8.— Specific frequency of ACs in dwarf satellite galaxies of M31 and the MW vs. luminosity (left panel) and metallicity (right panel) of the host systems. Blue filled circles are MW dwarfs. Red and green filled square are M31 satellites off and on the GPoA, respectively.

CMD appears to be heavily contaminated by MW foreground stars in the red part ($1.4 \leq B-V \leq 1.9$ mag) and by background unresolved galaxies in the blue part ($-0.1 \leq B-V \leq 0.1$ mag, see Section 9 in Paper I and e.g. Bellini et al. 2010; Bellazzini et al. 2011). In the right panel plot, red filled circles are RRab stars (58 sources), blue open circles are RRc stars (31 sources) and the green triangle is the AC. The RR Lyrae stars trace the HB, their distribution in apparent V mean magnitude is very broad ranging from 24.70 to 25.55 mag (see Figure 10). A most significant peak is observed at $\langle V(RR)\rangle \sim 25.25$ mag, followed by a second peak at $\langle V(RR)\rangle \sim 25.10$ mag.

The four panels in Figure 11 show the CMDs of sources in the 4 individual CCDs of the LBC mosaic (labeled C1, C2, C3 and C4). Similarly Figure 12 shows the distributions in apparent V mean magnitude of the RR Lyrae stars in C1, C2, C3 and C4, separately. Although contamination by foreground MW stars/background unresolved galaxies (see left panel of Figure 9) and broadening of both RGB and HB is present in each of the four individual CMDs, C3 shows a more prominent RGB extending as bright as $V \sim 22.5$ mag, whereas the RGB in the other 3 CCDs seems to be truncated around $V \sim 23.5$ mag. Furthermore, as shown by Figure 12 the peak at $\langle V(RR)\rangle \sim 25.25$ mag is mainly due to the RR Lyrae stars located in C3.

To investigate the spatial distribution of And XXVII stars we selected objects in the RGB region of the CMD obtained in the total LBC FoV (see left panel of Figure 9) with magnitude and color in the ranges of $22.5 \leq V \leq 25.3$ mag and $0.8 \leq B-V \leq 1.3$ mag, respectively. We built isodensity maps by binning these RGB stars in $1.2' \times 1.2'$ boxes and smoothing with a Gaussian kernel of $1.2'(0.02^{\circ})$ FWHM. The left panel of Figure 13 shows the RGB isodensity maps where the outermost contour levels are 3σ above the sky background. Interesting features are revealed by the isodensities contours of this selection. A high-counts isodensity contour shows up around Richardson et al. (2011)'s center coordinates of And XXVII. This region, named C in the figure, has been marked with a dotted circle of 4 arcmin in radius that is entirely contained into C2. The second isodensity has a very elongated structure that extends in south-east direction and reaches a second high-counts isodensity displaced by about 0.2 degrees in south-east direction from the center of the C region. This second region has been named SE and is marked by a dotted circle of 4 arcmin in radius with center coordinates: R.A.=$00^{\rm h}38^{\rm m}10.4^{\rm s}$, decl.=$+45^{\circ}21'34''$ that is entirely contained into C3. In both regions, SE and C, we adopted a radius of 4 arcmin that defines an area twice the high-counts isodensity contours. In the SE region there is a concentration of stars as high as in the C region and a higher number of RR Lyrae stars.

The presence of two high density contours in the map of Figure 13 points out that And XXVII has a very complex physical structure. We have to stress that the contamination of background and foreground sources can hamper the RGB stellar counts even if the selection was performed in the specific region of the CMD containing RGB stars at the distance of And XXVII (see left panel of Figure 9). Moreover, a complex physical structure of And XXVII is also corroborated by the wide RGB and the large spread in mean apparent magnitude of the RR Lyrae stars ($\langle V(RR)\rangle$) that can be attributed a distance spread. Three possible alternative scenarios to explain And XXVII's structure

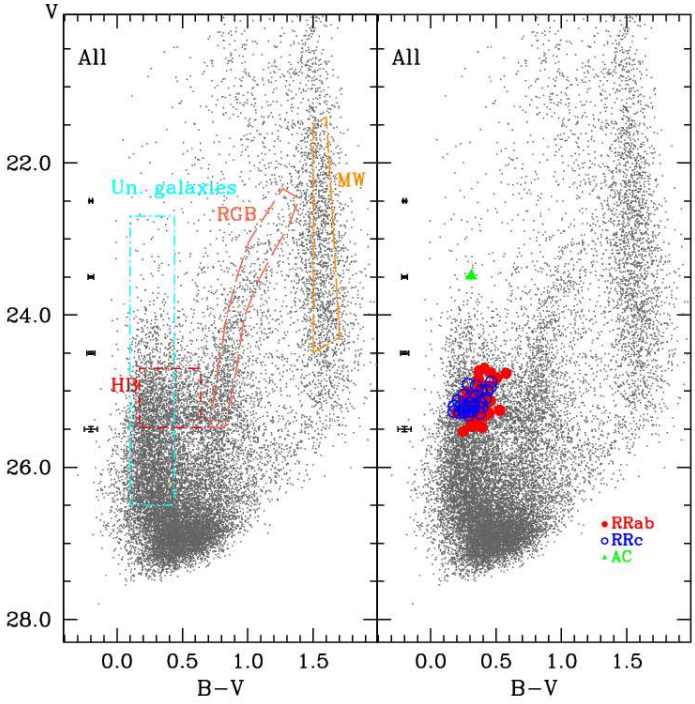

Fig. 9.— *Left*: CMD of the sources in the whole LBC FoV. Only objects with $-0.35 \leq$ Sharpness ≤ 0.35 and $\chi < 1.5$ are displayed. The RGB, HB and MW selections are marked with dashed regions. *Right*: Same as left but with superimposed the variable stars. Red filled circles are the RRab stars, blue open circles are the RRc stars and the green triangle is the AC.

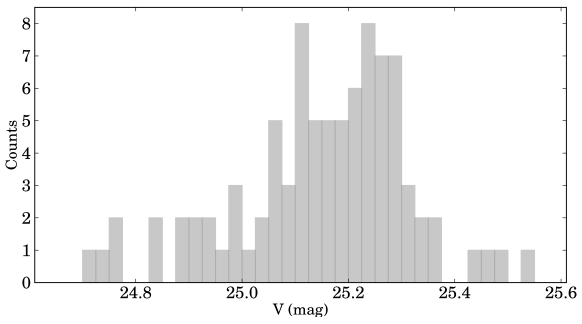

Fig. 10.— Distribution in apparent V mean magnitude of the 89 RR Lyrae stars identified in the field of And XXVII. The bin size is 0.025 mag.

and its two stellar concentrations are presented in Section 7. Isodensity contours were also computed selecting stars in the HB region ($25.6 \leq V \leq 24.6$ mag, $0.17 \leq B - V \leq 0.64$ mag) of And XXVII CMD, as shown in the right panel of Figure 13. The HB region of the CMD is contaminated by unresolved background galaxies (blue box, left panel of Figure 9), but still the HB stars well follow the structure traced by the RGB stars. We tried to select And XXVII's HB stars choosing objects closest to the CMD region defined by the RR Lyrae stars, but given the presence in this region of the CMD of unresolved background galaxies, the exact shape of the HB isodensities depends on the selection performed. For the RGB selection the contamination is not as crucial as for HB stars, indeed if we make multiple selections of the RGB region the shape of the isodensity contours does not change significantly. In order to characterize the stellar populations in the two isodensities with the highest stellar counts we drew the CMDs of the sources in the C and SE regions separately. The result is shown in Figure 14. The CMD of the SE region is similar to the CMD of C3 and shows a

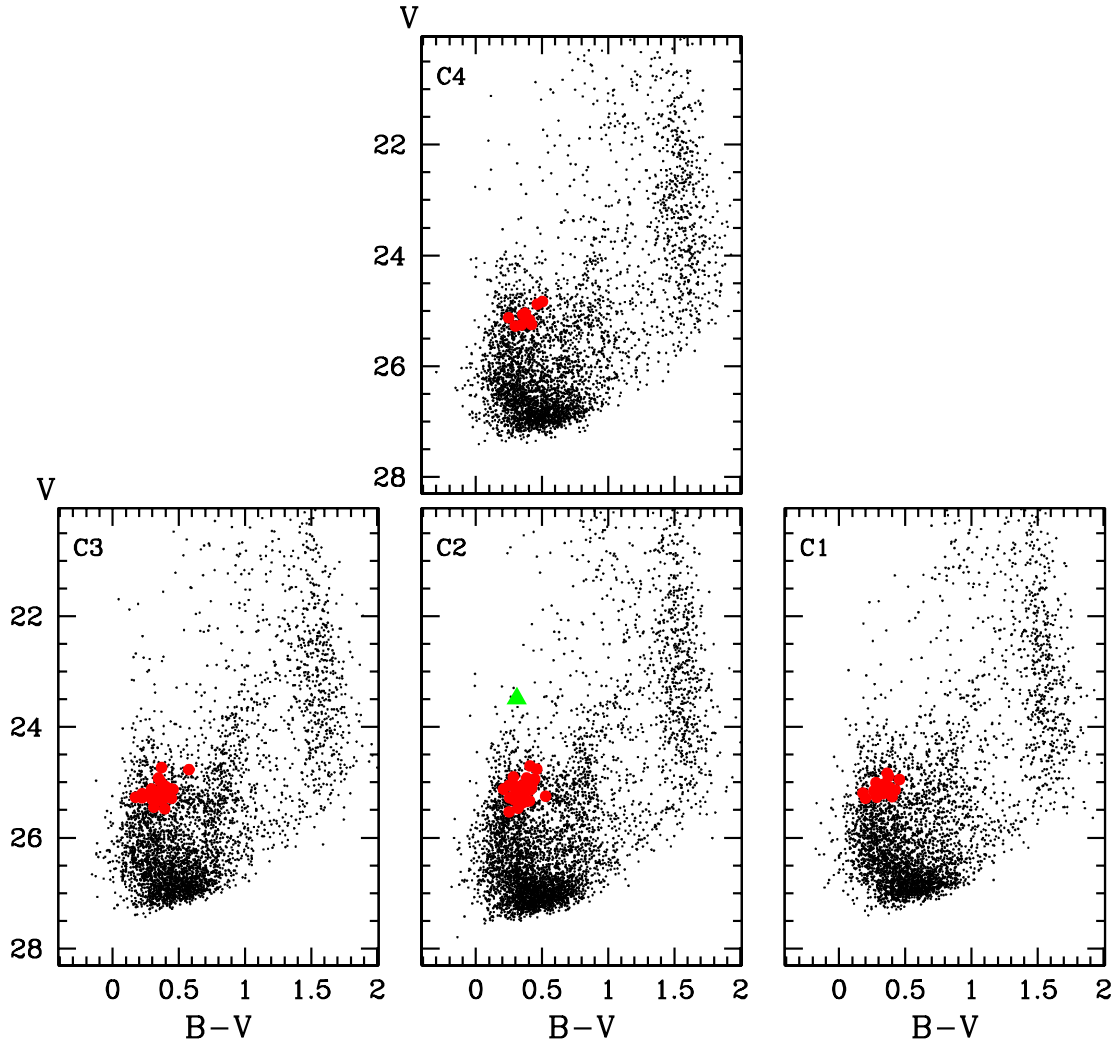

Fig. 11.— CMDs of sources in the 4 CCDs of the LBC mosaic. Only objects with $-0.35 \leq$ Sharpness ≤ 0.35 and χ <1.5 are displayed. Red filled circles are the RR Lyrae stars: 32 in C3, 29 in C2, 21 in C1 and 7 in C4. The green triangle is the AC which is located in C2.

well extended, better defined and narrower RGB especially around the tip, than the CMD of the C region which RGB appears instead truncated around $V \sim 23.5$ mag as also is the CMD of C2. The HB of SE is also better defined than that in region C. The lower panel of Figure 15 shows the distribution in apparent V mean magnitude of the 11 RR Lyrae stars in region C, while the upper panel shows the mean magnitude distribution of the 18 RR Lyrae stars in region SE. Fifteen of the 18 RR Lyrae stars contained in SE trace a rather tight HB with $\langle V(RR) \rangle = 25.24$ mag and $\sigma = 0.06$

mag (average on 15 stars). On the contrary, the 11 RR Lyrae stars of region C are rather spread in magnitude (see left panel of Figure 14 and bottom panel of Figure 15) with $\langle V(RR)\rangle$ = 25.15 mag and σ= 0.15 mag. This makes us wonder whether the actual center of And XXVII might be in the SE region rather than in C, as found by Richardson et al. (2011).

We have superimposed on the SE CMD an isochrone of 13 Gyr with [Fe/H]=-1.8 as derived from the web interface CMD 2.9[5] based on the Marigo et al. (2017) evolutionary tracks. The isochrone was corrected for the distance and reddening derived in Section 5 for the SE region. This isochrone well fits the position of RR Lyrae and RGB stars. The comparison between isochrone and observed CMD suggests a higher metallicity value for And XXVII than measured by Collins et al. (2013). The isochrone fit result is consistent (within the errors) with the metallicity estimated using the RR Lyrae stars in Section 3.2. A similar conclusion is also reached by comparison with the RGB and HB ridge lines of galactic Globular Clusters (GCs) with different metallicities, the best result is obtained for NGC 4147 with [Fe/H]=-1.8 dex (Harris 1996, 2010 edition). In the following we adopt [Fe/H]=-1.8 dex for the metallicity of And XXVII.

5. DISTANCE AND STRUCTURE

The mean luminosity of the RR Lyrae stars can be used to estimate the distance to And XXVII. We are aware that some of the RR Lyrae stars in the field of And XXVII can belong to the M31 halo, but since it is not possible to distinguish them, in deriving the distance we used all the sample of 89 RR Lyrae stars found in this work. The average V apparent magnitude of the 89 RR Lyrae stars in the field of And XXVII is $\langle V(RR)\rangle$=25.15 mag (σ=0.17 mag average on 89 stars). As in previous papers of this series we derived the reddening from the RR Lyrae stars adopting the method of Piersimoni et al. (2002, equation at page 1538). The reddening estimated in this way, $\langle E(B-V)\rangle = 0.04 \pm 0.05$ mag (where the error is the standard deviation of the mean), is slightly smaller but still consistent within 1 σ with the value inferred by Schlegel et al. (1998, $E(B-V) = 0.08 \pm 0.06$ mag). The visual absorption A_V was derived using the extinction law $A_V = 3.1 \times E(B-V)$ from Cardelli et al. (1989). We then adopt $M_V = 0.54 \pm 0.09$ mag for the absolute visual magnitude of RR Lyrae stars with metallicity [Fe/H] = -1.5 dex (Clementini et al. 2003) and $\frac{\Delta M_V}{\Delta [Fe/H]} = -0.214 \pm 0.047$ mag/dex (Clementini et al. 2003; Gratton et al. 2004) for the slope of the RR Lyrae luminosity-metallicity relation. For the metallicity of And XXVII we adopt [Fe/H]=-1.8 ± 0.3 dex as derived from isochrone fitting and consistent with the estimate from the RR Lyrae stars. The resulting distance modulus is (m-M)$_0$=24.55 ± 0.26 mag. This is 0.16 mag fainter but still consistent, within the large error, with Richardson et al. (2011) lower limit of $\geq$ 757 $\pm$ 45 kpc (corresponding to (m-M)$_0$=24.39 ± 0.13 mag) and placing And XXVII within the M31 complex. The faintest estimate by Conn et al. (2012): (m-M)$_0$=$25.49^{+0.07}_{-1.03}$ mag has a very large asymmetric error likely due to the difficulty in identifying the tip of RGB which is very scarcely populated in And XXVII. In any case, our estimate is consistent within the errors with the lower limit of Conn et al. (2012) estimate. The large error in our distance estimate is due in a good fraction to the significant dispersion of the average magnitude of the whole RR Lyrae star sample. As anticipated in Section 4, And XXVII appears to be in the process of tidal disruption, this may have resulted in the RR Lyrae stars to be located at different distances from us, thus causing the large dispersion in $\langle V(RR)\rangle$. To further investigate the galaxy structure we have compared number and properties of the RR Lyrae stars located in different parts of the LBC FoV starting from the two regions with highest stellar counts, namely, regions C and SE in Figure 13.

There are 18 RR Lyrae stars in the SE region and only 11 in the C region. This difference remains even if we reduce the radius of the two regions: in a circular portion of SE of 3 arcmin in radius there are 8 RR Lyrae stars to compare with 6 RR Lyrae contained in a same portion of region C. Average V magnitude, reddening and other characteristics (total number of RR Lyrae stars, average RRab period, distance modulus and fraction of RRc pulsators) for the RR Lyrae stars in region C and SE separately are provided in Table 3. Two sets of values are listed for region SE, the first

[5] $http://stev.oapd.inaf.it/cgi-bin/cmd$

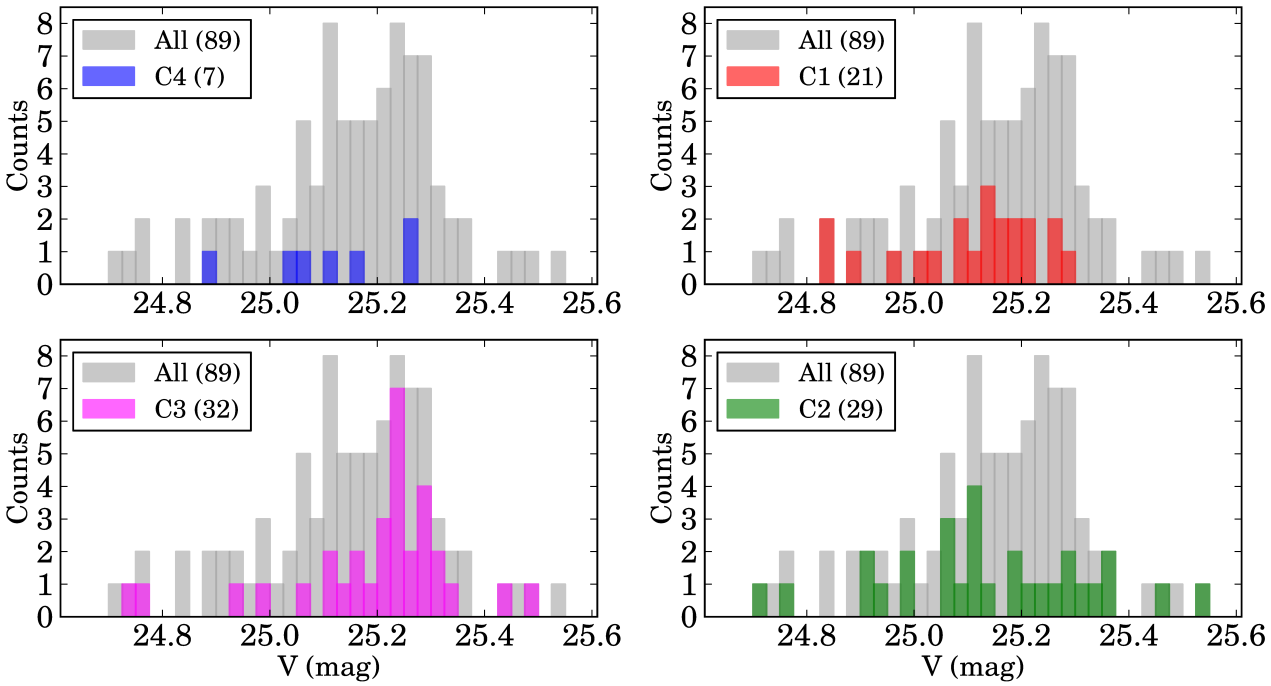

Fig. 12.— Distribution in apparent V mean magnitude of the RR Lyrae stars in the 4 CCDs of the LBC mosaic. The bin size is 0.025 mag.

one corresponding to the whole set of 18 variables, and the second one (labeled SE1 in the table) considering only the 15 RR Lyrae stars whose mean magnitude peaks around $\langle V \rangle \sim 25.24$ mag. Distance moduli of C and SE differ by 0.08 mag in the first case, this difference is still within 1 σ given the large dispersion of the estimates. The difference is of 0.21 mag in the second case (SE1) and may be due to a real radial distance effect. However, considering the large errors we are dealing with, this conclusion has to be taken with caution. The spread in magnitude can be due to a real three-dimensional (3D) effect, but not as big as 0.21 mag. The centers of regions C and SE are ~ 0.2 degree a part in the sky, that at the distance of And XXVII corresponds to a physical projected separation of ~ 3 kpc. Is this an indication that the galaxy is disrupted and the SE component is 3 kpc away from the galaxy center? Or, since SE has the cleanest CMD and the largest concentration of RR Lyrae stars most of which are located approximately at the same distance from us, could SE be the remaining nucleus of the now disrupted And XXVII?

Triggered by these two different possibilities we divided the RR Lyrae stars in two samples, corresponding, respectively, to the south and north portions of And XXVII according to Richardson et al. (2011) center coordinates. Characteristics of the RR Lyrae stars in the north and south samples are also summarized in Table 3. North and south distance moduli differ by ~ 0.2 mag, that although still consistent within the respective errors could indicate a 3D effect where the north part of And XXVII is closer to us than the south part.

We also tested whether possible zero point differences among the four CCDs of the LBC might cause the observed differences, by comparing the median apparent B and V magnitudes of objects in the blue part ($-0.1 \leq B - V \leq 0.1$ mag, $24 \leq V \leq 26$ mag) and in the red part ($1.6 \leq B - V \leq 1.9$ mag, $23 \leq V \leq 25$ mag) of the CMD.

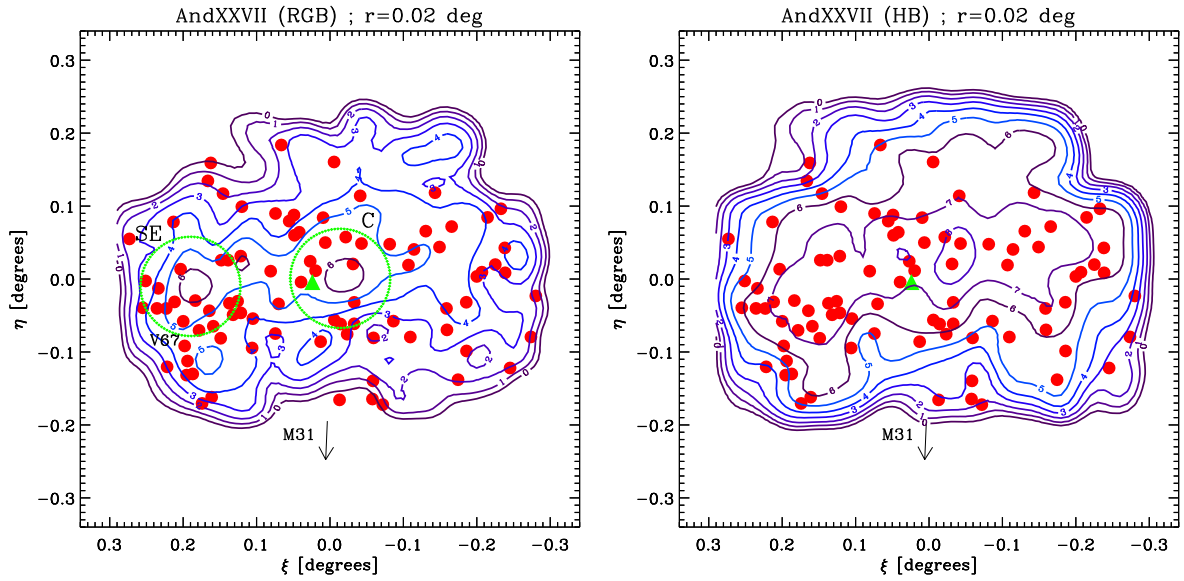

Fig. 13.— *Left*: Isodensity contours of RGB stars in And XXVII. X and Y axes are, respectively, RA and decl. differential coordinates computed from the center of the galaxy given by Richardson et al. (2011). Red filled circles are RR Lyrae stars, the green filled triangle is the AC. We have labeled the RR Lyrae star V67 for which we have estimated a metallicity of [Fe/H]=−1.86 ∼ 0.50 dex (on the Carretta et al. 2009 scale) from the Fourier parameter ϕ_{31}. The green circles mark areas of 4 arcmin in radius around regions C and SE, respectively. *Right*: Same as in the left panel but for And XXVII HB stars.

Differences among the 4 CCDs range from 0.001 to 0.03 mag both in the B and V bands, hence cannot explain the difference observed between average apparent magnitudes of the north and south RR Lyrae subsamples. Similarly, these differences cannot be explained by differential reddening, as reddening is generally small and very similar among the various RR Lyrae subsamples. We computed also the average reddening derived from the RR Lyrae stars in the four CCDs obtaining: $\langle E(B-V)\rangle_{C1} = 0.03 \pm 0.06$ mag, $\langle E(B-V)\rangle_{C2} = 0.03 \pm 0.06$ mag, $\langle E(B-V)\rangle_{C3} = 0.05 \pm 0.05$ mag and $\langle E(B-V)\rangle_{C4} = 0.01 \pm 0.06$ mag. Therefore we conclude that the magnitude differences are real and likely due to a 3D effect. Figure 16 shows the spatial distribution of the 89 RR Lyrae stars in the field of And XXVII, where each source is color-coded according to its mean apparent magnitude ($\langle V\rangle$). If we assume that differences in $\langle V\rangle$ values are totally due to a projection/distance effect, which is sensible given the similarity of pulsation properties of the 89 RR Lyrae stars and the low and homogeneous reddening in the area, the distribution in Figure 16 suggests that And XXVII center likely is in the SE overdensity and the galaxy is tilted with the north-west portion closer to us than the south-east part.

We recall that among the three other M31 satellites we observed with the LBT, we did not find evidence of a particular smearing in mean magnitude of the RR Lyrae stars in And XIX and And XXV, whereas the magnitude spread observed in And XXI was found to be fully justified by the presence of two RR Lyrae populations with different metallicities as also suggested by the bi-modal period distribution of the RRab stars (see Figure 2 in Paper II). However, the scatter of the RR Lyrae star mean magnitude in the field of And XXVII is over twice than observed in And XXI, while there is no evidence of bi-modality in period of the RRab stars. This along with the large spread in the spatial distribution of the RR Lyrae population make us to conclude that either we are resolving the 3D structure of a galaxy in the final stage of disruption or we are sampling the RR Lyrae stars in And XXVII together with those in a background/foreground structure like

Table 3: Properties of selected samples of RR Lyrae stars in And XXVII.

id	N (RRab+RRc)	$\langle V(RR)\rangle$	$\langle P_{ab}\rangle$	$\langle P_c\rangle$	E(B-V)	$(m-M)_0$	f_c
ALL	58+31	25.15 ± 0.17	0.59 ± 0.05	0.35 ± 0.04	0.04 ± 0.05	24.55 ± 0.26	0.35
SE	9+9	25.17 ± 0.17	0.58 ± 0.05	0.35 ± 0.03	0.05 ± 0.05	24.54 ± 0.26	0.50
SE1	6+9	25.24 ± 0.06	0.55 ± 0.01	0.35 ± 0.03	0.03 ± 0.05	24.67 ± 0.20	0.60
C	6+5	25.15 ± 0.15	0.62 ± 0.03	0.33 ± 0.05	0.07 ± 0.05	24.46 ± 0.25	0.45
NORTH	29+15	25.09 ± 0.16	0.60 ± 0.04	0.36 ± 0.04	0.05 ± 0.03	24.46 ± 0.22	0.35
SOUTH	29+16	25.20 ± 0.15	0.59 ± 0.05	0.34 ± 0.04	0.03 ± 0.06	24.63 ± 0.27	0.35

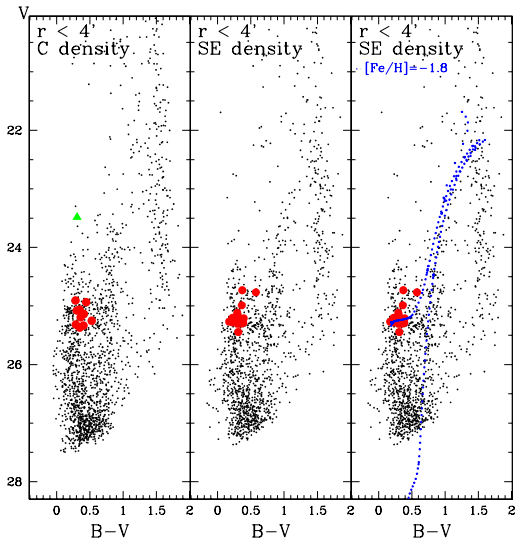

Fig. 14.— *Left*: CMD of sources in the C overdensity region. *Center*: Same as in the left panel, but for the SE region. *Right*: CMD of the SE region with superimposed an isochrone of 13 Gyr with [Fe/H]=−1.8 dex (blue dotted line; see text for details).

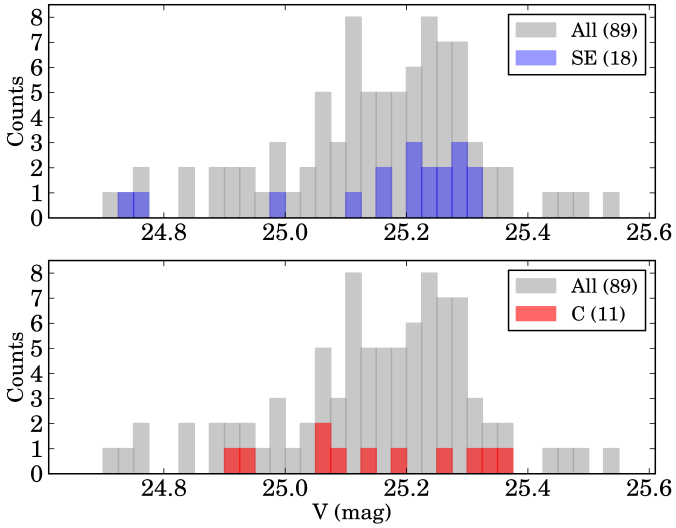

Fig. 15.— *Lower panel*: Distribution in apparent V mean magnitude of the 11 RR Lyrae stars in the C region. *Upper panel*: Same as in the lower panel, but for the 18 RR Lyrae stars in the SE region.

the M31 NW stream or the M31 halo.

5.1. Different old stellar populations?

If the differences in magnitudes of the RR Lyrae star subsamples are not due to distance effects a possible alternative explanation is the presence in And XXVII of different old stellar generations. To test this hypothesis the positions on the CMD of the different samples of RR Lyrae stars listed in Table 3 were compared to the model of Marconi et al. (2015) and the 13 Gyr isochrones of Marigo et al. (2017) after correction for the reddening and the distance modulus derived using our whole RR Lyrae stars sample [$(m-M)_0$=24.55 ± 0.26 mag, $\langle E(B-V)\rangle = 0.04 \pm 0.05$ mag]. To further constrain the observations we compared also the observed period distribution of the RRab pulsators to the models. Starting from the C sample the position on the CMD and the period distribution of the RRab can be reproduced by the models with metallicity from $[Fe/H] = -2.3$ to -1.5 dex, M=0.67-0.8 $M_\odot$, T_eff=5900-6900 K and LogL=1.69-1.79 $L_\odot$. The $[Fe/H] = -1.5$ models are at the limit of the redder RR Lyrae stars.

The SE sample appears on average bluer and fainter that the best matching models with metallicity from $[Fe/H] = -2.3$ to -1.7 dex, M=0.716-

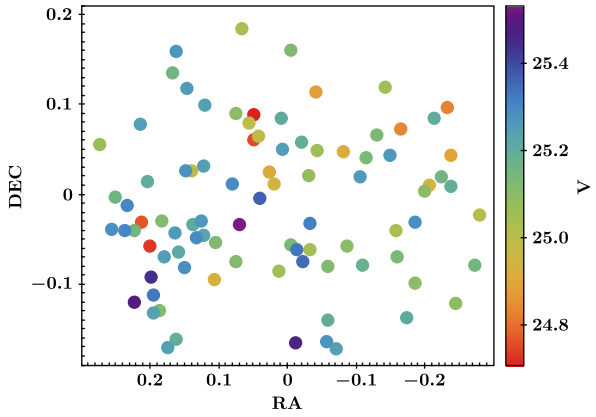

Fig. 16.— Spatial distribution of the RR Lyrae stars in the field of And XXVII. Stars are color-coded according to their mean V magnitude.

0.8 $M_\odot$, T_eff=6000-6900 K and LogL=1.72-1.76 $L_\odot$ Moreover the observed distribution in periods of the SE RRab sample is shorter that the one derived from the latter models. Indeed models more metal rich than $[Fe/H] = -1.8$ are too red to reproduce the color of the RRab stars. The observations are only matched if we correct the models for the distance modulus and reddening found for the SE1 sample [$(m\text{-}M)_0$=24.67 ± 0.26 mag, $\langle E(B-V)\rangle = 0.03 \pm 0.05$ mag]. We concluded that the scenario for which the RR Lyrae stars have same metallicities, but different distances is best matched by the models as shown in the right panel of Figure 17. In this case both the RR Lyrae stars and the RGB stars are well reproduced by the 13 Gyr isochrones with a $[Fe/H] = -1.8$ corrected for the distance moduli $(m-M)_0$=24.46 mag and $(m-M)_0$=24.67 mag, that represent the extreme values reported in Table 3. The twofold RR Lyrae population can thus not be explained by the presence of two generations of stars with different metallicity at the same distance. The simple old stellar generation placed at different distances has to be preferred over the double stellar population (see right panel of Figure 17). We are maybe sampling two different regions in the M31 halo, one belonging to And XXVII and the other to the NW stream that is in the back/front of And XXVII (see Section 6).

6. Association with the North-West stream

The NW stream is a stellar structure extending up to 120 kpc from the center of M31, that in its arc-path intersects And XXVII. This stream was first detected by Richardson et al. (2011), in the PandAS map of metal poor ([Fe/H]< -1.4 dex) RGB stars. The mean surface brightness of the NW stream is 28-29 mag arcsec^{-2} and the estimated total mass is $\sim 10^7$ $M_\odot$ (Carlberg et al. 2011). In the literature a mass of M=$8.3^{+2.8}_{-3.9}$ $\times 10^7 M_\odot$ was estimated for And XXVII by Collins et al. (2013) using the velocity dispersion, under the assumption that the galaxy is in dynamical equilibrium and is spherically symmetric. However both assumptions are very uncertain given the clearly disrupted nature of this galaxy. A very rough mass estimate inferred from the total number of RR Lyrae stars would place And XXVII in the class of 10^7 $M_\odot$ dwarf galaxies, like And I or And VI (see Table 4 for the number of RR Lyrae stars in these galaxies and the masses in Collins et al. 2014).

Projected along the NW stream are also seven GCs. Veljanoski et al. (2014) measured their radial velocity (RV) finding that six of them show a clear trend with the projected distance from the M31 center, velocities being more negative as the GCs approach the M31 center. Monte Carlo simulations performed by Veljanoski et al. (2014) showed that these six GCs are physically associated among them (with an average RV of -430 ± 30 km s^{-1}) and with the NW stellar stream. Given its position along the stream, And XXVII has a RV compatible with that found for the GCs assuming a quasi-circular inclined orbit where the direction of rotation goes from west to east for the objects in the NW stream. And XXVII maybe be the satellite galaxy that generated the NW stream. The galaxy is perhaps completing a full orbit around M31 and after a near pericenter passage started losing stars. However, with the current data set we can not definitively prove this hypothesis. More kinematic and photometric data are needed to investigate the likely connection between the NW stream and And XXVII.

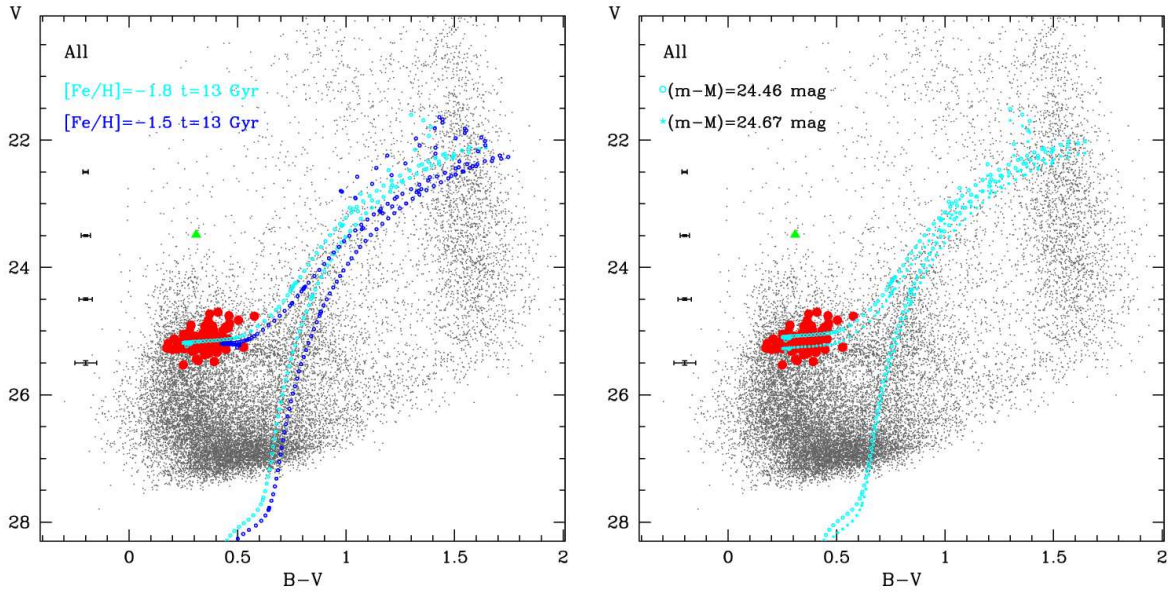

Fig. 17.— *Left*: Same as Figure 9 with superimposed the 13 Gyr isochrones from Marigo et al. (2017) with $[Fe/H] = -1.8$ dex (cyan line) and $[Fe/H] = -1.5$ dex (blue line). *Right*: Same as in the left panel, but with the same isochrone of 13 Gyr and $[Fe/H] = -1.8$ corrected for distance moduli of (m-M)=24.46 mag (upper line) and (m-M)=24.67 mag (lower line), respectively.

7. COMPARISON WITH OTHER M31 SATELLITES AND CONCLUSIONS

Following the procedure in Paper III we compared the pulsation properties of the RR Lyrae populations in the M31 dSph satellites on and off the GPoA. Table 4 summarizes the characteristics of the pulsating variable stars in the M31 dSphs that have been studied so far for variability, 11 in total. Six of them are on and five are off the GPoA.We computed the average period of the RRab stars for galaxies on and off the plane separately, finding $\langle P_{ab}\rangle$=0.60±0.07 d and $\langle P_{ab}\rangle$=0.60 ± 0.06 d. The fraction of RRc to total number of RR Lyrae stars is f_c=0.27 and f_c=0.23 for on and off plane satellites, respectively. Hence, both samples are compatible with an Oo-Int classification and show a slight tendency to Oo I type as the galaxies get closer to M31 (see also right panel of Figure 5). The cumulative period distribution of the RR Lyrae stars in the two samples is shown in Figure 18. A two sample Kolmogorov-Smirnov (K-S) test to check whether there are any differences between the two populations returns a p-value of p= 0.03209, meaning that the two RR Lyrae populations differ significantly. The two samples differ especially in the short period regime (P< 0.4 d, see Figure 18). This is mainly due to the large number of short period RR Lyrae stars in And XXVII (indeed the p value in Paper III was p=0.36, that is without the RR Lyrae stars of And XXVII). The fraction of RRc stars in And XXVII is oddly high. A similar result was found by Brown et al. (2004) in some fields of the M31 halo. These authors measured a fraction f_c=0.46, an average period for RRab of $\langle P_{ab}\rangle$=0.594 d and an average period for RRc of $\langle P_c\rangle$=0.316 d. Between Brown et al. (2004) results and ours in And XXVII (see Table 3) there are some similarities like the average period of RRab and the high fraction of RRc. Furthermore, the right panel of Figure 5 shows a similar trend of the period-amplitude diagram of M31 halo and And XXVII RR Lyrae stars. These analogies can be translated in three possible scenarios: 1) a number of the RR Lyrae stars in the field of And XXVII do in fact belong to the M31 halo (the projected distance of And XXVII from the M31 center is $d_p \sim 60$ kpc) and in par-

ticular to the NW stream. This would explain the spread in distance we observe from the RR Lyrae stars; 2) And XXVII is not a dwarf galaxy but rather an overdensity in the NW stream (as claimed by Martin et al. 2016) that is largely composed by M31 halo stars; 3) And XXVII is the progenitor of the NW stream and part of the M31 halo. The high concentration of RR Lyrae stars and the CMD of And XXVII SE region, along with the possible connection with the GCs in the NW stream seem to support this latter possibility. However, as shown in Figure 9 of Ibata et al. (2014) the M31 halo in And XXVII neighborhood is very complex and the stars into the metallicity range $-2.5 < [Fe/H] < -1.7$ dex are placed in streams located all around And XXVII. Investigation of the variable stars and CMD of the area beyond the SE region in the south-east direction, as well as in different regions of the M31 halo and NW stream is essential in order to discern among the above different scenarios.

Concerning the frequency of ACs in the M31 satellites, with the discovery of only one AC in And XXVII we confirm the finding of Paper III that on-plane satellites seem to host only a few or none ACs. There are 4 ACs in total in the 6 on-plane satellites in Table 4 to compare with 21 ACs in the 5 off-plane systems. This would suggests that only off-plane satellites were able to retain enough gas to give rise to an intermediate-age stellar population and produce ACs. In this regard, the recent detection of an irregularly shaped HI cloud close to but offset from the stellar body of And XIX (Kerp et al. 2016) and of some HI emission displaced by half a degree from And XXI (Kerp private communication), gives support to the possible presence of a 1-2 Gyr old stellar generation in And XIX and And XXI, and being both these systems off the GPoA, maybe in the off-plane M31 satellites in general.

We warmly thank P. Montegriffo for the development and maintenance of the GRATIS software. Financial support for this research was provided by PRIN INAF 2010 (PI: G. Clementini) and by Premiale LBT 2013. The LBT is an international collaboration among institutions in the United States, Italy, and Germany. LBT Corporation partners are The University of Arizona on behalf of the Arizona university system; Istituto Nazionale di Astrofisica, Italy; LBT Beteiligungsgesellschaft, Germany, representing the Max-Planck Society, the Astrophysical Institute Potsdam, and Heidelberg University; The Ohio State University; and The Research Corporation, on behalf of The University of Notre Dame, University of Minnesota, and University of Virginia. We acknowledge the support from the LBT-Italian Coordination Facility for the execution of observations, data distribution, and reduction. Facility: LBT

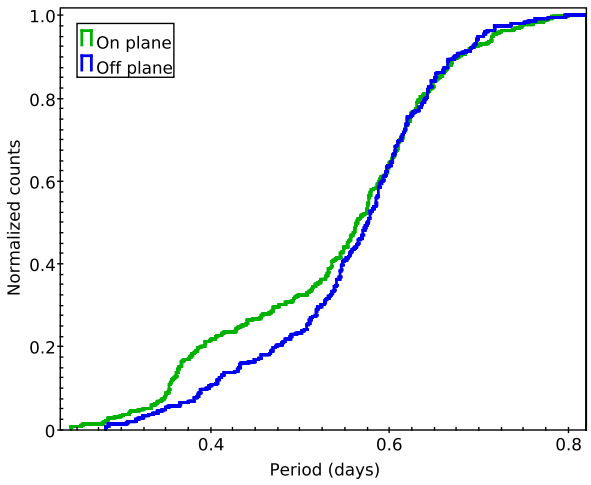

Fig. 18.— Cumulative period distribution of the RR Lyrae stars in M31 satellite galaxies on and off the GPoA.

REFERENCES

Alcock, C., Allsman, R. A., Alves, D. R. et al. 2000, AJ, 119, 2194

Annibali, F., Nipoti, C., Ciotti, L., et al. 2016, ApJ, 826, L27

Bailey, S. I. 1902, Annals of Harvard College Observatory, 38, 1

Bellazzini, M., Beccari, G., Oosterloo, T. A., et al. 2011, A&A, 527, A58

Bellini, A., Bedin, L. R., Piotto, G., et al. 2010, A&A, 513, A50

Brown, T. M., Ferguson, H. C., Smith, E., et al. 2004, AJ, 127, 2738

Table 4: Properties of the variable stars in the Andromeda satellite galaxies

Name	N (RRab+RRc)	$\langle P_{ab} \rangle$	f_c	N (AC)	N (AC) confirmed*	member (GpoA)	Reference
And I	72+26	0.57	0.26	1?	0	yes	(1)
And II	64+8	0.57	0.11	1	0	no	(2)
And III	39+12	0.66	0.23	5?	2	yes	(1)
And VI	91+20	0.59	0.18	6	4	no	(3)
And XI	10+5	0.62	0.33	0	0	yes	(4)
And XIII	12+5	0.66	0.30	0	0	yes	(4)
And XVI	3+6	0.64	0.33	0	0	no[1]	(5,6)
And XIX	23+8	0.62	0.26	8	8	no	(7)
And XXI	37+4	0.63	0.10	9	9	no	(8)
And XXV	46+11	0.60	0.19	2	1	yes	(9)
And XXVII	58+31	0.59	0.35	1	1	yes	(10)

* confirmed AC, based on the Period-Weseneheit relation (see Paper III)

[1] offset by 8 Kpc from the Great Plane of Andromeda (GPoA, Ibata et al. 2013)

(1) Pritzl et al. (2005); (2) Pritzl et al. (2004); (3) Pritzl et al. (2002);

(4) Yang & Sarajedini (2012); (5) Mercurio et al. (2017, in preparation);(6) Monelli et al. (2016);

(7) Cusano et al. (2013); (8) Cusano et al. (2015);(9) Cusano et al. (2016); (10) this work

Bullock, J. S., & Johnston, K. V. 2005, ApJ, 635, 931

Cacciari, C., Corwin, T. M., & Carney, B. W. 2005, AJ, 129, 267

Cardelli, J. A., Clayton, G. C., Mathis, J. S.1989, ApJ, 345, 245

Carlberg, R. G., Richer, H. B., McConnachie, A. W. et al. 2011, ApJ, 731, 124

Carretta, E., Bragaglia, A., Gratton, R. G., et al. 2009, A&A, 505, 117

Catelan, M. 2009, Ap& SS, 320, 261

Clement, C. M., & Rowe, J. 2000, AJ, 120, 2579

Clementini, G., Di Tomaso, S., Di Fabrizio, L., et al. 2000, AJ, 120, 2054

Clementini, G., Gratton, R., Bragaglia, et al. 2003, AJ, 125,1309

Clementini, G. 2010, Variable Stars, the Galactic halo and Galaxy Formation,

Collins, M. L. M., Chapman, S. C., Rich, R. M., et al. 2013, ApJ, 768, 172

Collins, M. L. M., Chapman, S. C., Rich, R. M., et al. 2014, ApJ, 783, 7

Conn, A. R., Ibata, R. A., Lewis, G. F., et al. 2012, ApJ, 758, 11

Cusano, F., Clementini, G., Garofalo, A., et al. 2013, ApJ, 779, 7

Cusano, F., Garofalo, A., Clementini, G., et al. 2015, ApJ, 806, 200

Cusano, F., Garofalo, A., Clementini, G., et al. 2016, ApJ, 829, 26

Gratton, R. G., Bragaglia, A., Clementini, G., et al. 2004, A&A, 421, 937

Harris, W.E. 1996, AJ, 112, 1487

Ibata, R. A., Lewis, G. F., Conn, A. R., et al. 2013, Nature, 493, 62

Ibata, R. A., Lewis, G. F., McConnachie, A. W. et al. 2014, ApJ, 780, 128

Jacyszyn-Dobrzeniecka, A. M., Skowron, D. M., Mróz, P., et al. 2016, AcA, 66, 149

Jeffery, E. J., Smith, E., & Brown, T. M. et al. 2011, AJ, 141, 171

Jurcsik, J., & Kovacs, G. 1996, A&A, 312, 111

Kapakos, E., Hatzidimitriou, D., & Soszyński, I. 2011, MNRAS, 415, 1366

Kerp, J., Kalberla, P. M. W., Ben Bekhti, N., et al. 2016, A&A, 589A, 120

Marconi, M., Fiorentino, G., & Caputo, F. 2004, A&A, 417, 1101

Marconi, M., Coppola, G., Bono, G., et al. 2015, ApJ, 808, 50

Marigo, P., Girardi, L., Bressan, A., et al. 2017, ApJ, 835, 77

Martin, N. F., Ibata, R. A., McConnachie, A. W., et al. 2013, ApJ, 776, 80

Martin, N. F., Ibata, R. A., Lewis, G. F. et al. 2016, arXiv:1610.01158

Monelli, M., Martnez-Vzquez, C. E., Bernard, E. J. et al. 2016, ApJ, 819, 147

Oosterhoff, P. T. 1939, The Observatory, 62, 104

Pawlowski, M. S., Kroupa, P., Jerjen, H., et al. 2013, MNRAS, 435, 1928

Piersimoni, A. M., Bono, G., & Ripepi, V. 2002, AJ, 124, 1528

Pritzl, B. J., Armandroff, T. E., Jacoby, G. H., & Da Costa, G. S. 2002, AJ, 124, 1464

Pritzl, B. J., Armandroff, T. E., Jacoby, G. H., & Da Costa, G. S. 2004, AJ, 127, 318

Pritzl, B. J., Armandroff, T. E., Jacoby, G. H., & Da Costa, G. S. 2005, AJ, 129, 2232

Richardson, J. C., Irwin, M. J., McConnachie, A. W., et al. 2011, ApJ, 732, 76

Ripepi, V., Marconi, M., Moretti, M. I., et al. 2014, MNRAS, 437, 2307

Sarajedini, A., Mancone, C. L., Lauer, T. R., et al. 2009, AJ, 138, 184

Schlegel, D. J., Finkbeiner, D. P., & Davis, M. 1998, ApJ, 500, 525

Simon, N. R., & Teays, T. J. 1982, ApJ, 261, 586

Stetson, P. B. 1987, PASP, 99, 191

Stetson, P. B. 1994, PASP, 106, 250

Stierwalt, S., Liss, S. E., Johnson, K. E., et al. 2017, Nature Astronomy, 1, 0025

Veljanoski, J., Mackey, A. D., Ferguson, A. M. N., et al. 2014, MNRAS, 442, 2929

Yang, S.-C. & Sarajedini, A. 2012,MNRAS, 419, 1362

This 2-column preprint was prepared with the AAS LaTeX macros v5.2.